

Interfacial Electron Transfer in Metal Cyanide-Sensitized TiO₂ Nanoparticles[†]

James A. Harris, Kevin Trotter, and Bruce S. Brunschwig*

Molecular Materials Research Center, Beckman Institute, MC 139-74, California Institute of Technology, 1200 East California Boulevard, Pasadena, California 91125

Received: November 29, 2006; In Final Form: January 17, 2007

Electroabsorption (Stark) spectroscopy has been used to study the charge-transfer absorption from a transition-metal–cyanide complex to a TiO₂ nanoparticle. Transition-metal cyanide/TiO₂(particle) systems were synthesized using Fe^{II}(CN)₆^{4−}, Ru^{II}(CN)₆^{4−}, Mo^{IV}(CN)₈^{4−}, and W^{IV}(CN)₈^{4−}. On formation of the M(CN)_{*n*}^{4−}/TiO₂(particle) system, a new metal-to-particle charge-transfer (MPCT) absorption band is observed in the 390–480 nm region. Analysis of the absorption spectra suggests that the TiO₂ level involved in the MPCT transition resides at significantly higher energy than the bottom of the conduction band and that the electronic coupling between the two metal centers is the dominant factor determining the position of the MPCT band maximum. The average charge-transfer distances determined by Stark spectra range from 4.1–4.7 Å. The observation of relatively short charge-transfer distances leads to the conclusion that the MPCT absorption is from the transition-metal cyanide center to a level that is localized on the Ti atom bound to a nitrogen end of the [O₂Ti–N–C–M(CN)_{*x*}] system. The electronic coupling, *H*_{ab}, calculated for a two state model is similar to values observed in dinuclear metal complexes.

Introduction

Charge-transfer processes at semiconductor–electrolyte interfaces are presently of considerable interest with significant effort directed toward both a fundamental understanding of the factors that control the kinetics^{1–5} and spectroscopy of charge transfer^{6–8} and the development of alternatives to solid-state photovoltaic devices for solar-to-electrical energy conversion.⁹ An example of such a device is the dye-sensitized (Grätzel-type) solar cell (DSSC),^{10–12} where a dye, usually a transition-metal complex, absorbs a photon of visible light to produce an excited state that then injects an electron into the conduction band of a wide-band gap semiconductor film, usually composed of nanoparticles of TiO₂. The absorption spectra of the dye/TiO₂ system are normally the sum of the individual spectra of the dye and the TiO₂ semiconductor. As a consequence, the dye and the semiconductor are believed to interact weakly. Despite the weak interaction, the electron transfer from the dye to the semiconductor usually takes place on the femto- and picosecond timescales.¹⁰ For a number of dyes a second type of sensitization is possible. In these systems the dye interacts more strongly with the semiconductor and a new absorption band, ascribable to charge transfer from the dye to the semiconductor, is observed.¹³ Thus, the absorption of a photon results in the creation of an electron in the TiO₂ particle and an oxidized dye.

The two types of charge-transfer reactions at semiconductors can be viewed as parallel to the thermal and optical electron-transfer processes observed between two metal centers connected by a bridging ligand. For a purely thermal electron-transfer reaction, “hot” electron transfer is unlikely to occur because there are no electrons in higher vibrational levels, due to the unfavorable Boltzmann factor. However, in DSSCs, the electron transfer from the excited state is so rapid that many of the

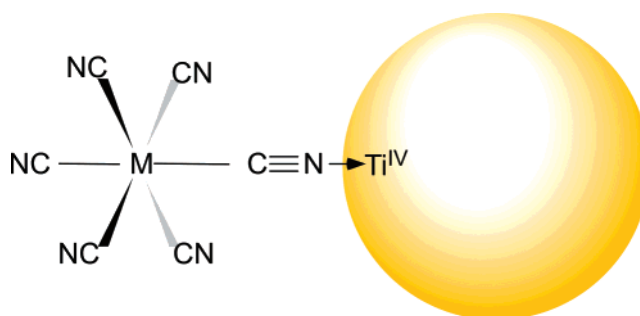


Figure 1. Schematic illustration of a M(CN)_{*n*}^{4−}/TiO₂(particle) system.

injected electrons have not had time to thermally relax, to either the singlet or the triplet state of the excited dye, and “hot” electron transfer accounts for a significant portion of the transferred electrons.

Colloidal TiO₂ nanoparticles and metal–cyanide ions are known to form charge-transfer complexes at low pH as indicated by the formation of a new absorption band at 420 nm. The Fe(CN)₆^{4−}/TiO₂ system has been studied by UV–vis,^{14,15} photocurrent,^{14–17} Raman,^{18,19} infrared,^{18,20,21} and electroabsorption spectroscopy,²² as well as by flash photolysis.^{13,23} The iron complex is believed to bind at a surface Ti^{IV} site via a monodentate cyanide ligand, (CN)₅Fe^{II}–CN–Ti^{IV}(particle) (Figure 1).^{18,19} The new absorption observed for metal–cyanide complexes bound to TiO₂ at 400–500 nm has been assigned as a metal-to-particle charge-transfer (MPCT) transition. Electron injection into the semiconductor by the iron complex has been shown to occur in less than 50 fs.^{13,23} The very rapid injection together with the new CT absorption band supports the hypothesis that the optical absorption involves direct charge transfer from the iron to the TiO₂ nanoparticle.

Stark spectroscopy allows one to study the optical charge-transfer process and to characterize the distance of the charge transfer. We have previously studied the MPCT in the Fe(CN)₆^{4−}/TiO₂ system.²² That study found that the charge-transfer

[†] Part of the special issue “Norman Sutin Festschrift”.

* E-mail: bsb@caltech.edu.

distance is independent of the size of the TiO₂ particle. We showed that, in the case of the Fe(CN)₆⁴⁻/TiO₂ system, the charge transfer involves the transfer of an electron from the iron center to the Ti atom that is coordinated to the N end of the bridging CN group.

Time-dependent density functional theory (TD-DFT) studies have provided support for the assignment of the transition as a Fe(II)-to-TiO₂ charge transfer.²⁴ The calculation assigns the initial and final states of the charge transfer to states that are largely localized on the Fe(II) and the Ti(IV) to which the Fe(CN)₆⁴⁻ is coordinated, respectively. Studies of TiO₂ functionalized by catechol and other organic donors also show the development of a new absorption band to the red of the band gap,^{25,26} and DFT calculations assign the absorption to a charge-transfer transition from the catechol to the TiO₂.²⁷

According to the standard model, an electron injected into a nanoparticle initially enters the conduction band and is then trapped in local sites within the particle. Normally conduction-band states are considered to be delocalized across many semiconductor atoms. The MPCT band generated on complex-particle formation allows the use of electroabsorption (Stark) spectroscopy to study the charge-transfer transition. Stark spectroscopy affords a unique way of characterizing the initially formed charge-transfer state by providing information on the distance of the initial charge transfer and the changes in dipole-moment and polarizability between the ground and Franck–Condon states and the electronic coupling between the states. For the direct-injection mechanism, this should elucidate whether, in the Franck–Condon state, the electron is in a conduction-band state delocalized across the entire particle or in a state localized on an individual titanium center.

Experimental

All chemicals were obtained from Aldrich except K₄[W^{IV}(CN)₈]·H₂O and K₄[Mo^{IV}(CN)₈]·2H₂O, which were kindly donated by Professor Harry B. Gray. The ≈2 nm TiO₂ nanoparticles were prepared according to a literature procedure.²² Briefly, titanium(IV) propoxide (4 mL) was dissolved in anhydrous 2-propanol (10 mL). The resulting solution was added rapidly (in one shot) to a mixture containing water (10 mL), ethylene glycol (10 mL), and concentrated HCl (2 mL) under vigorous stirring to give a clear solution. After 1 h of stirring, the volatiles were removed by rotary evaporation under vacuum at 60 °C. The residue was dissolved in 0.5 M HCl (10 mL) to give a clear colloid solution.

Preparation of M(CN)_n⁴⁻/TiO₂(particle) Solutions. TiO₂ nanoparticle colloid (0.7 M TiO₂, 0.25 M HCl, 50:50 water–ethylene glycol) solutions were mixed with K₄[M(CN)_n] solutions according to Table 1. The K₄[M(CN)_n] solutions were added dropwise with vigorous stirring (to avoid agglomeration) to the TiO₂ colloid solution to produce colored solutions. It was found that slow dropwise addition was necessary in order to avoid agglomeration of the M(CN)_n⁴⁻/TiO₂(particle) systems. These solutions were used soon after preparation. The pH of the solution was calculated from the HCl concentration in the TiO₂ solution and the volumes used.

UV–Vis Spectroscopy. UV–vis spectra were obtained using an Agilent 8453 diode array spectrophotometer. Spectra of the M(CN)_n⁴⁻/TiO₂ systems were recorded in 50:50 water–ethylene glycol. The TiO₂ colloid solution (0.5 mL) prepared as above was diluted to 10 mL with 50:50 water–ethylene glycol. This dilute solution (2 mL) was placed in a 1 cm quartz cuvette, and a ca. 25 mM solution of M(CN)₆⁴⁻ in 50:50 water–ethylene glycol was titrated in. After each addition, the cuvette

TABLE 1: Mixing Volumes and Concentrations for M(CN)_n⁴⁻/TiO₂ Systems

M(CN) _n ⁴⁻	[M] mM	V(M(CN) _n ⁴⁻) mL	V(TiO ₂) mL	[M(CN) _n ⁴⁻] ^a mM	pH ^b
Fe ^{II} (CN) ₆ ⁴⁻	24.8	0.7	0.5	14.5	1
Ru ^{II} (CN) ₆ ⁴⁻	25.3	0.7	0.5	14.8	1
Mo ^{IV} (CN) ₈ ⁴⁻	88.4	0.2	0.5	25.3	0.5
W ^{IV} (CN) ₈ ⁴⁻	78.3	0.2	0.5	22.4	0.5

^a Metal cyanide concentration in final solution. ^b pH of the final solution estimated from the volumes and concentrations used.

was shaken to ensure good mixing and allowed to settle, and a spectrum was recorded. Additional aliquots were added until the absorption of the MPCT band was ≈1.5.

Stark Spectroscopy. The Stark spectrometer, experimental methods, and data analysis procedure were as previously reported,^{28–30} except that a Xe arc lamp was used as the light source in the place of a W filament bulb. The glassing medium was 50:50 water–ethylene glycol, for which the local field correction f_{int} is estimated as 1.33.²⁹

The zeroth, first, and second derivatives of the absorption spectrum were used for analysis of the electroabsorption $\Delta\epsilon(\nu)$ spectrum in terms of the Liptay treatment.^{31,32} For a fixed randomly orientated sample, the Liptay equation is

$$\Delta\epsilon(\nu)/\nu = \left[A_{\chi}\epsilon(\nu)/\nu + \frac{B_{\chi}}{15h} \frac{\partial(\epsilon(\nu)/\nu)}{\partial\nu} + \frac{C_{\chi}}{30h^2} \frac{\partial^2(\epsilon(\nu)/\nu)}{\partial\nu^2} \right] F_{\text{int}}^2 \quad (1)$$

where ν is the frequency of the light in Hz, h is the Planck constant, and the internal electric field is related to the applied external field by $F_{\text{int}} = f_{\text{int}}F_{\text{ext}}$. The coefficients, A_{χ} , B_{χ} , C_{χ} , are dependent on the angle between the electric field in the sample and the polarization of the light, χ .

$$C_{\chi} = C_1 + [3(\cos(\chi))^2 - 1]C_2$$

The observed adiabatic dipole-moment change for the CT transition, $\Delta\mu_{12}$, is given by

$$|\Delta\mu_{12}| = \sqrt{C_1/5}$$

$$|m\Delta\mu_{12}| = \sqrt{C_2/3 + C_1/15}$$

A two-state (diabatic/adiabatic) analysis of the MLCT transitions gives

$$\Delta\mu_{\text{ab}}^2 = \Delta\mu_{12}^2 + 4\mu_{12}^2 \quad (2)$$

where the subscripts 1 and 2 indicate the adiabatic states, a and b indicate diabatic states, and μ_{12} is the observed transition dipole-moment determined from the oscillator strength f_{os} of the transition by

$$|\mu_{12}| = [f_{\text{os}}/(1.08 \times 10^{-5}h\nu_{\text{max}})]^{1/2} \quad (3)$$

where $h\nu_{\text{max}}$ is the energy of the MLCT maximum (in wave-numbers). The degree of delocalization c_b^2 and electronic coupling matrix element H_{ab} for the diabatic states are given by

$$c_b^2 = \frac{1}{2} \left[1 - \left(\frac{\Delta\mu_{12}^2}{\Delta\mu_{12}^2 + 4\mu_{12}^2} \right)^{1/2} \right] \quad (4)$$

$$|H_{ab}| = \left| \frac{E_{\max}(\mu_{12})}{\Delta\mu_{ab}} \right| \quad (5)$$

If the trace of the polarizability change, $\text{Tr}(\Delta\alpha)$, is much larger than a term that is a product of the polarizabilities and the normalized transition moments^{33,34} then

$$\text{Tr}(\Delta\alpha) = \frac{2}{5} B_1 \quad (6)$$

Results and Discussion

UV–Vis Spectroscopy. On formation of the $\text{M}(\text{CN})_n^{4-}/\text{TiO}_2$ - (particle) systems (TiO_2 nanoparticles ≈ 2 nm), a new absorption band appeared in the 390–480 nm region. Absorption spectra of the $\text{M}(\text{CN})_n^{4-}/\text{TiO}_2$ (particle) and TiO_2 recorded in 50:50 water–ethylene glycol at room temperature are presented in Figure 2. The corresponding spectral data are presented in Table 2.

The molar absorptivities of the MPCT bands (based on the metal cyanide concentration) of the Fe and Mo systems were in good agreement with previous measurements.¹⁵ However, the MPCT band for the $\text{Ru}(\text{CN})_6^{4-}/\text{TiO}_2$ system was present only as a shoulder precluding an accurate determination of the molar absorptivity at the band maximum. The $\text{W}(\text{CN})_8^{4-}/\text{TiO}_2$ system yielded a molar absorptivity that does not agree with earlier work;¹⁵ it is consistent, however, with the value for the $\text{Mo}(\text{CN})_8^{4-}/\text{TiO}_2$ system. This suggests either that some of the $\text{W}(\text{CN})_8^{4-}$ in our systems is not bound to the TiO_2 nanoparticles or that the earlier extinction coefficient is wrong.

The $\text{Fe}(\text{CN})_6^{4-}/\text{TiO}_2$ (particle) system is well characterized with the absorption assigned as a MPCT transition. The absorptions in the other systems are similarly assigned as MPCT transitions on the basis of the similarity of their properties to those of the iron system (see below).

Recently a model for charge-transfer transitions from a molecular redox center to the conduction band of a semiconductor has been developed.^{6,8} The model assumes that the ground and excited states of the system can be described by parabolic energy surfaces and that the population of the systems in the ground state is Boltzmann. In the case of the $\text{M}(\text{CN})_n^{4-}/\text{TiO}_2$ system we are considering, the parabolic surfaces are the result of changes in the nuclear coordinates of the cyanide system. The excited state of the system involves a particular level, i , in the conduction band of the semiconductor. The distribution of systems per unit of energy difference between the states is given by

$$n_A = \frac{[C_0]}{\sqrt{4\pi\lambda k_B T}} \exp\left[-\frac{(\lambda + \Delta G_{b,i}^0 - h\nu)^2}{4\lambda k_B T}\right] \quad (7)$$

where n_A is the concentration of systems per unit energy that have an energy difference between the ground and excited state equal to the photon energy $h\nu$, λ is the reorganization energy of the system, C_0 is the concentration of CT systems present, $\Delta G_{b,i}^0$ is the free-energy change for the transfer of an electron to the i -th level of the conduction band in the CT complex (in our systems, the transfer is from the metal–cyanide complex bound to the semiconductor), k_B is the Boltzmann constant, and T is the temperature. If we assume that the probability of photon absorption is independent of the ground-state energy, then the molar absorptivity for the CT absorption to a level i of the

semiconductor, $\epsilon_{v,i}$, is given by

$$\frac{\epsilon_{v,i}}{\nu} \propto \frac{(\mu_{12,i})^2}{\sqrt{\pi\lambda k_B T}} \exp\left\{-\frac{(\lambda + \Delta G_{b,i}^0 - h\nu)^2}{4\lambda k_B T}\right\} \quad (8)$$

where $\epsilon_{v,i}$ is the molar absorptivity for the individual transition and $\mu_{12,i}$ is the transition moment of the individual absorption to level i . The free-energy change is given by

$$\begin{aligned} \Delta G_{b,i}^0 &= \epsilon_i^{\text{CB}} + E_{\text{CB}} + eE_b^{\text{or}} \\ &= \epsilon_i^{\text{CB}} + \Delta G_b^0 \end{aligned} \quad (9)$$

where E_{CB} is the energy of the bottom of the conduction band, ϵ_i^{CB} is the energy of the i -th level relative to the bottom edge, E_b^{or} is the reduction potential for the donor bound to the TiO_2 , e is the charge on the electron, and ΔG_b^0 is the standard free-energy change for transfer of an electron from the bound donor to the bottom of the conduction band.

Equation 8 is a Gaussian function for $\epsilon_{v,i}/\nu$ as a function of the energy of the absorbed photon, $h\nu$. The maximum of the Gaussian for the absorption to level i has an energy, $h\nu_{\max,i}$, of (Figure 3)

$$h\nu_{\max,i} = \epsilon_i + \lambda + \Delta G_b^0 \quad (10)$$

The individual transition moment, $\mu_{12,i}$, is given by a Mulliken–Hush type of expression:

$$\mu_{12,i} = (H_{ab,i} e r_i / \nu_{\max,i}) \quad (11)$$

where $H_{ab,i}$ is the electronic coupling between the donor and the semiconductor and r_i is the distance over which the electron transfer occurs.

The total absorption, ϵ_v/ν , is then the summation of the individual absorptions:

$$\begin{aligned} \frac{\epsilon_v}{\nu} &= \int_0^\infty \frac{\epsilon_{v,i}}{\nu} \rho^{\text{CB}} d\epsilon_i^{\text{CB}} \propto \int_0^\infty \frac{(\mu_{12,i})^2}{\sqrt{\pi\lambda k_B T}} \times \\ &\quad \exp\left\{-\frac{(\lambda + \epsilon_i^{\text{CB}} - h\nu + \Delta G_b^0)^2}{4\lambda k_B T}\right\} \rho^{\text{CB}} d\epsilon_i^{\text{CB}} \end{aligned} \quad (12)$$

where ρ^{CB} is the density of state (DOS) of the conduction band.

When the DOS of the TiO_2 is constant and the transition moment is given by a Mulliken–Hush expression, eq 11, the total absorption is predicted to have a peak at^{6–8}

$$h\nu_{\max} = \Delta G_b^0 + \lambda + \sqrt{4\lambda k_B T} \quad (13)$$

The free-energy change for electron transfer can be estimated from

$$\Delta G_b^0 = E_{\text{cb}} + eE_{\text{M}(\text{CN})_n^{4-}}^{\text{or}} + k_B T \ln(K_{\text{red}}/K_{\text{ox}}) \quad (14)$$

where $E_{\text{M}(\text{CN})_n^{4-}}^{\text{or}}$ is the formal reduction potential of the free metal complex in solution and the last term is the ratio of the binding constants for the metal–cyanide complex to the semiconductor in its reduced and oxidized forms. The ratio of the binding constants corrects the driving force for differences in the energy required to bring and bind the complexes to the semiconductor. The reduction potentials for the complexes in water are shown in Table 2. The ratio of the binding constants has been estimated to be $\approx 10^4$ (10^2 to 10^5).¹⁷ This gives a value

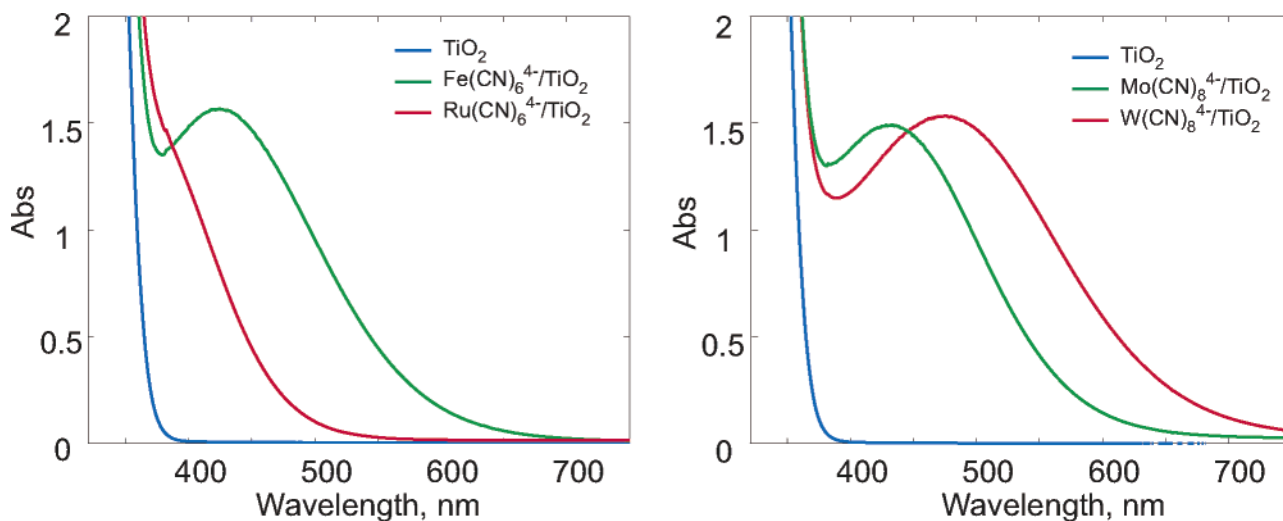


Figure 2. Absorption spectra of $M(CN)_n^{4-}/TiO_2$ (particle) systems (red/blue) and TiO_2 (black) recorded in 50:50 water–ethylene glycol at room temperature.

TABLE 2: UV–Vis Spectroscopic Data for $M(CN)_4^{4-}/TiO_2$ Systems in 50:50 Water–Ethylene Glycol

$M(CN)_n^{4-}$	λ_{max}^a nm	ϵ_{max}^b $M^{-1} cm^{-1}$	E_{red}^c V	ΔG_b^d eV	$\lambda_{max,calc}^{d,e}$ nm	$\lambda_{max,calc}^{d,f}$ nm
$Fe^{II}(CN)_6^{4-}$	430	5000	0.36	0.50	700	530
$Ru^{II}(CN)_6^{4-}$	390	sh	0.86	1.00	540	440
$Mo^{IV}(CN)_8^{4-}$	438	1300	0.73	0.87	580	460
$W^{IV}(CN)_8^{4-}$	480	1500	0.46	0.60	660	510

^a Room temperature. ^b Calculated on the basis of the metal cyanide concentration. ^c vs NHE ref 35. ^d Calculated from eq 14 using $E_{cb} \approx -0.1$ eV and $k_B T \ln(K_{red}/K_{ox}) = 0.24$ eV. ^e Calculated from eq 13 using $\lambda = 1.0$ eV. ^f Calculated using eqs 13 and 14 with $\lambda = 1.0$ eV, $E_{cb} = +0.4$ eV, and $k_B T \ln(K_{red}/K_{ox}) = 0.24$ eV.

for $k_B T \ln(K_{red}/K_{ox})$ of 0.24 ± 0.1 eV. The reorganization energy, λ , is estimated as ≈ 1 eV^{8,17,36} (see discussion below), and the conduction-band energy of TiO_2 ($E_{cb} = -eE_{fb}$, where E_{fb} is the flat band potential of the TiO_2) is pH-dependent and is estimated to be ≈ -0.1 V vs NHE at pH 1.^{37,38} Using these values, we estimated ν_{max} to be at significantly lower energy than the observed absorption maxima (Table 2).

If the peak of the absorption occurs for charge transfer not into the lowest level of the conduction band but rather into a state ≈ 0.5 eV above the conduction-band edge, then the predicted and observed band maxima are in much better agreement (Table 2). A TD-DFT study for the $Fe(CN)_6^{4-}/TiO_2$ system shows this behavior and predicts that, although the lowest energy absorption is at 1.7 eV, the peak of the absorption band occurs at ≈ 2.8 eV (450 nm), close to that observed.²⁴

The model for the MPCT transition also allows one to calculate a band shape for the absorption.^{6–8} Modeling of the MPCT spectra suggests that to reproduce the rise in the absorbance profile on the low-energy side of the MPCT bands for the Fe, Mo, and W systems it is necessary to use reorganization energies of ≈ 1.0 eV and a ΔG^0 that is increased by ≈ 0.5 eV (Figure 4). The reorganization energy and free-energy change values that give agreement between the observed and calculated spectra are not well defined, and a range of values ($\approx \pm 0.3$ eV) is possible. A reorganization energy of 1.0 eV is larger than one normally observes for either thermal or optical CT between molecular centers when there are no contributions from bond-length changes in the complex.^{39,40}

The outer-sphere reorganization energy for the transfer of an electron from a donor to a semiconductor acceptor can be

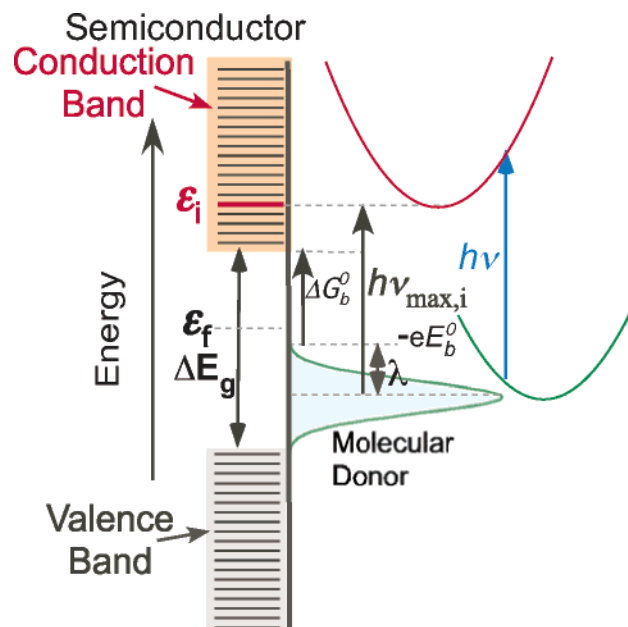


Figure 3. Distribution function of the dye and a semiconductor particle shown with the parabolic energy surfaces for the ground and excited state of the system. The band gap is ΔE_g , E_b^0 is the reduction potential of the bound dye, ΔG_b^0 is the free-energy for transferring an electron, ϵ_f is the Fermi level, and ϵ_i is the energy of the level that receives the electron.

estimated from⁴¹

$$\lambda = \frac{(\Delta q)^2}{8\pi\epsilon_0} \left\{ \frac{1}{a} \left(\frac{1}{D_{op,sol}} - \frac{1}{D_{s,sol}} \right) - \frac{1}{2r} \left[\left(\frac{D_{op,sc} - D_{op,sol}}{D_{op,sc} + D_{op,sol}} \right) \left(\frac{1}{D_{op,sol}} \right) - \left(\frac{D_{s,sc} - D_{s,sol}}{D_{s,sc} + D_{s,sol}} \right) \left(\frac{1}{D_{s,sol}} \right) \right] \right\} \quad (15)$$

where Δq is the amount of charge transferred; $D_{op,sc}$ and $D_{s,sc}$ are the optical (refractive index squared) and static dielectric constants of the semiconductor particle, respectively; $D_{op,sol}$ and $D_{s,sol}$ are the optical and static dielectric constants of the solution, respectively; r is the distance between the metal center and the surface of the particle; a is the radius of the metal–cyanide complex; and ϵ_0 is the permittivity of free space. Using standard molecular models,⁴² we estimated that the radius of the metal–

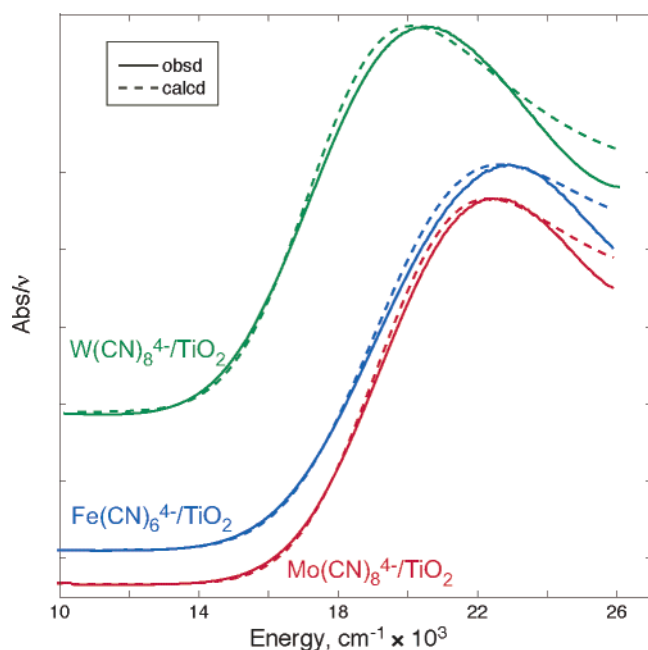


Figure 4. Observed (solid line) and calculated (dashed line) normalized absorption spectra of Fe (blue), Mo (red), and W (green) $M(CN)_n^{4-}/TiO_2$ at room temperature in 50:50 water–ethylene glycol. Calculated using λ and ΔG^0 values of 1.00, 1.4; 1.32, 1.1; and 1.16, 1.0 eV for the Fe, Mo, and W systems, respectively. Spectra are offset for clarity.

cyanide complex, a , is 5 Å. If the metal–cyanide complex is assumed to bind with the N end of the cyanide to a Ti atom on the surface of the particle, then r is ≈ 5 Å. The reorganization energy estimated from eq 15 for electron transfer from the metal cyanide to the TiO_2 particle (index of refraction (anatase) = 2.49, dielectric constant = 85)⁴³ is ≈ 0.6 eV, a value smaller than that suggested by the model of the MPCT absorption.

Gaal and Hupp have suggested a reorganization energy of ≈ 1.4 eV for the interfacial back electron transfer from SnO_2 to a series of ruthenium and osmium complexes electrostatically bound to a SnO_2 particle,^{44,45} and Kuciauskas et al.⁴⁶ estimate reorganization energies in the range 0.7–1.2 eV for the back reaction between a TiO_2 nanoparticle film and surface-coordinated ruthenium and osmium complexes from the temperature dependence of the rate constant. These large values of the reorganization energy observed for electron transfer between nanoparticles and metal complexes provides support for the use of large reorganization energies for the systems discussed here.

Although the MPCT spectrum is well modeled for the Fe, Mo, and W systems (Figure 4) on the low-energy side, the observed spectrum declines more sharply at high energy than the modeled spectrum. The model assumes that the charge-transfer absorption will take place to all the conduction-band states of the semiconductor, which results in a band shape that declines slowly with energy after the peak. The observed spectra for these systems are more symmetric around the peak and suggest that it is not well-modeled as a CT transition from a discrete molecular level to a continuum of conduction-band states that have both a constant DOS and an electronic coupling to the donor that is a simple function of the absorbance energy. Rather, it suggests that only a few conduction-band states contribute to the MPCT absorption and that these states are significantly above the energy of the band edge. Unfortunately, for all these systems, the TiO_2 absorption obscures the high-energy side of the band.

The injection of electrons into states well above the conduction-band edge is expected when either the density of states (DOS) of the semiconductor is not a constant but increases sharply with energy above the conduction-band edge and/or when the electronic coupling between the conduction-band states and the metal complex is a function of the injection level i . In general, the DOS for the conduction band is expected to rise proportionately to the $\sqrt{\epsilon}$, where ϵ is the energy above the conduction-band edge.⁴⁷ Calculations of the electronic structure of anatase TiO_2 regularly show a DOS that rises sharply from the band edge to give a series of peaks that range from 0.5 to 2 eV above the edge.^{48,49} Thus, one may assume that the maximum in the conduction-band DOS would occur at an energy significantly above the band edge.

Alternatively, or in addition, the electronic coupling between the metal–cyanide center and the conduction-band states is not expected to be independent of energy. States having a significant portion of their electron density on the Ti(IV) coordinated to the metal–cyanide complex would be more strongly coupled to the metal–cyanide center than states that have their density spread throughout the nanoparticle. In a nanoparticle, one might expect that the square of the electronic coupling would scale inversely with the number of semiconductor metal centers over which the state is delocalized.⁵⁰ Further, the Stark spectra (see below) of the metal–cyanide/ TiO_2 systems suggest that the absorption results in the transfer of an electron from the metal to the titanium atom attached to the nitrogen of the cyanide ligand bridging the two centers. In that case, it is probable that the coupling is much larger between the donor and conduction-band states that have a large contribution from that Ti atom than to more delocalized states. The maximum in the absorption spectra would then occur at an energy corresponding to these states. The observed Stark spectra suggest that it is this coupling that dominates the spectra.

TD-DFT calculations²⁴ of the $Fe(CN)_6^{4-}/TiO_2$ system show that both of these effects contribute to the band maximum: the DOS, as indicated by the number of transitions predicted, increases with energy; however, the most intense transitions have their final state localized on the Ti atom that is coordinated to the $Fe(CN)_6^{4-}$ ion. Thus, for the systems studied here, we estimate that the states localized on the Ti atoms are not the lowest level in the conduction band but rather 0.5–1 eV above the band edge.

Stark Spectroscopy. Representative MPCT absorption, electroabsorption, and electroabsorption spectral components for the $M(CN)_n^{4-}/TiO_2$ (particle) systems are shown in Figure 5. The electroabsorption spectra were modeled in terms of a large second-derivative component, a somewhat smaller first-derivative component, and a negligible zeroth-derivative contribution. The parameters resulting from the spectral fitting are presented in Table 3. The results for the $Fe(CN)_6^{4-}/TiO_2$ system are very close to those observed previously.²²

The second-derivative line shapes are interpreted as due to dipole-moment changes between ground and excited states.^{29,31} The dipole-moment changes gave a charge-transfer distance ($r_{12} = |\Delta\mu_{12}|/e$) of 4.1–4.7 Å. The distance for the $Fe(CN)_6^{4-}/TiO_2$ system has been shown to be independent of the size of the nanoparticle.²² Correcting the distances for the mixing between the two adiabatic states,³² $r_{ab} (=|\Delta\mu_{ab}|/e)$, increases the distance by only $\approx 2\%$, less than the error in the measurements. The distances are also somewhat less than the distance from the metal–cyanide center to a Ti(IV) coordinated to the N end of one of the cyanides, 5.1–5.3 Å, estimated from molecular modeling of the systems. These distances are much shorter than

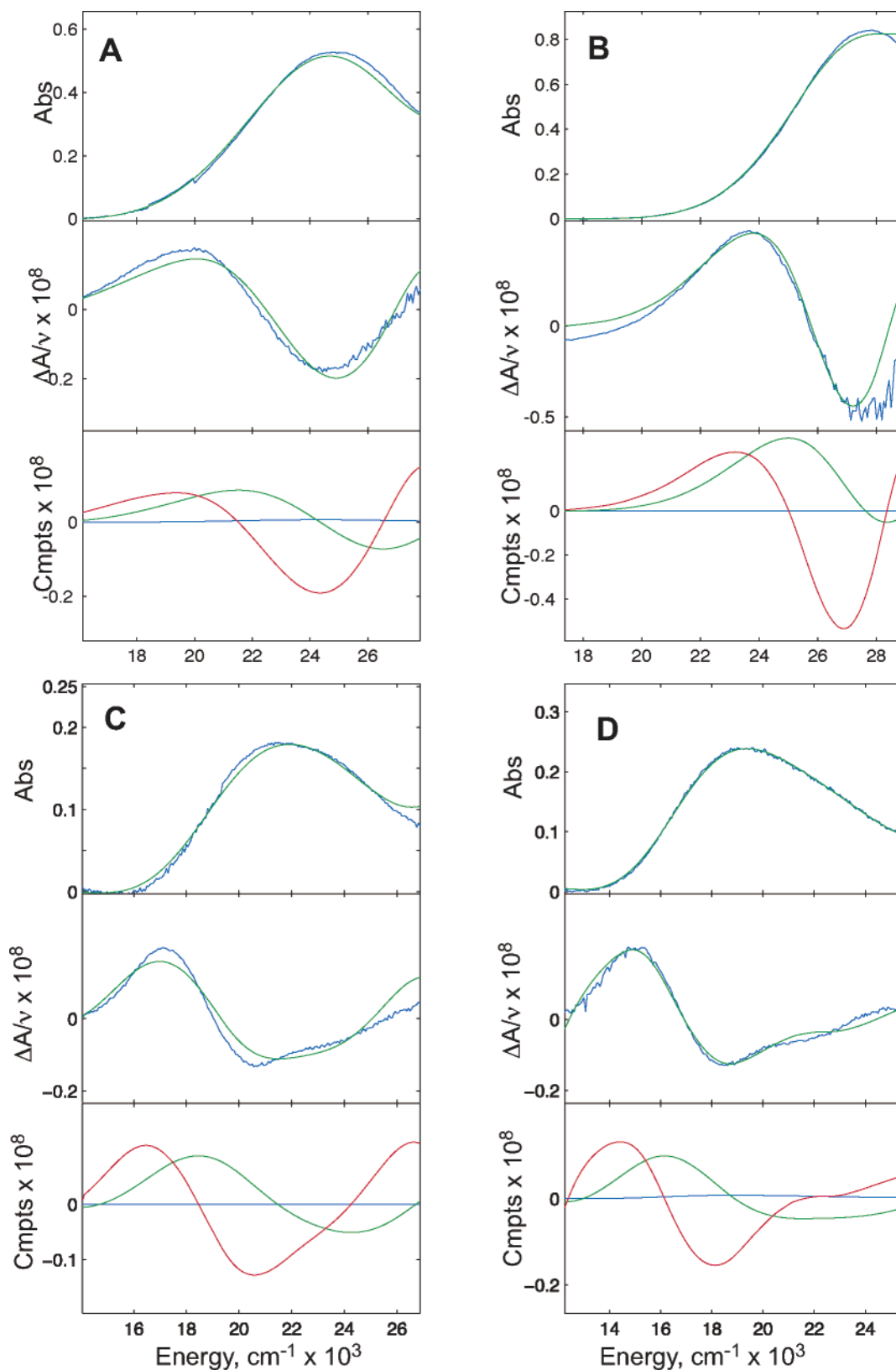


Figure 5. MPCT absorption, electroabsorption, and electroabsorption spectral components for $M(CN)_4^-/TiO_2$ (particle) systems ($M = Fe, A; Ru, B; Mo, C; W, D$) at 77 K in 50:50 water–ethylene glycol and a field strength of 1.76, 2.11, 2.12, and 1.77×10^3 V/m. In the top panel for each, the blue curve is the observed absorbance and the green is the smoothed spectra. In the middle panel, the blue curve is the observed Stark spectra and the green is the fit of the derivatives of the absorbance spectra to the observed spectra. In the bottom panel are shown the components of the fit weighted by their coefficients of the fit. The blue, green, and red curves are the zero-, first-, and second-derivative contributions of the fit spectra.

expected if the electron were transferred from the center of the metal–cyanide complex to an orbital delocalized over the whole of the TiO_2 particle. A charge transfer to a delocalized orbital

on a 20 Å diameter nanoparticle would have a charge-transfer distance of ≈ 15 Å. This finding suggests that the direct charge injection is from the metal center to an orbital primarily residing

TABLE 3: Spectral Data and Stark Fitting Results for $M(CN)_n^{4-}/TiO_2$ Systems at 77 K in 50:50 Water–Ethylene Glycol

$M(CN)_n^{4-}$	$h\nu_{\max, 77K}^{-1} \times 10^3$ cm ⁻¹	$ \mu_{12} $ eÅ	$ \Delta\mu_{12} ^a$ eÅ	$ \Delta\mu_{ab} $ eÅ	H_{ab}^b cm ⁻¹ × 10 ³	$Tr(\Delta\alpha)^c$ Å ³	$c_b^2 d$
Fe ^{II} (CN) ₆	24.9	0.7	4.7	5.0	3.8	600	0.02
Ru ^{II} (CN) ₆	28.9	0.6	4.1	4.2	4.3	700	0.02
Mo ^{IV} (CN) ₈	21.9	0.4	4.5	4.6	1.9	1000	0.01
W ^{IV} (CN) ₈	19.4	0.5	4.6	4.7	2.2	800	0.01

^a The estimated uncertainties are $\approx 15\%$. ^b Electronic-coupling element between the charge-transfer centers. ^c Polarizability change between the ground and excited states (50% uncertainty). ^d Degree of delocalization between the charge-transfer centers.

on one or a few titanium centers that are close to the point of attachment of the $M(CN)_n^{4-}$ moiety and not into a delocalized conduction-band state.

The emissive Stark spectrum for a coumarin-343 attached to TiO_2 particles (10 nm) has been observed.⁵¹ Although the results are not unequivocal, the observed $|\Delta\mu|/f_{\text{int}}$ of 3.9 eÅ yields a charge-transfer distance of 3.0 Å ($f_{\text{int}} = 1.33$). This distance is somewhat shorter than that observed here for the CT absorption of the $M(CN)_n^{4-}/TiO_2$ system. If the emission originates from a CT transition, which transfers an electron from the TiO_2 to the coumarin, then the initial state must be localized on a Ti atom that is at the point of coumarin attachment to the particle. Unfortunately, the data does not rule out the possibility that the emission arises from more prosaic processes centering on aggregation or surface environmental effects.⁵¹

Compared to most cyanide-bridged dinuclear systems, the Stark-derived charge-transfer distances and the polarizability changes, $\Delta\alpha$, found for the $TiO_2/M(CN)_n^{4-}$ systems are larger.^{33,52–55} Two cyanide-bridged dinuclear compounds, $[(CN)_5Fe^{II}-CN-Ru^{III}(NH_3)_4py]^-$ and $[(CO)_5Cr^{II}-CNRu^{III}(NH_3)_5]^{2+}$,^{33,52} have charge-transfer distances and polarizability changes similar to those found in the $M(CN)_n^{4-}/TiO_2(\text{particle})$ systems. This suggests that when the excited state is more polarizable than the ground state, larger charge-transfer distances are observed.

In general, the charge-transfer distances observed using Stark spectroscopy are shorter than the geometric distance between the putative redox centers. This has been interpreted as due to polarization effects of the two states.^{30,32} For most complexes, the donor center will be relatively more positive in the charge-transfer excited state than it was in the ground state. Therefore, if the polarizability of two states is the same, the system will be relatively more polarized toward the donating center in its excited state. This polarization produces a dipole-moment change that is opposite to the direction of the dipole-moment change due to the transferring electron and in an observed dipole-moment change that is smaller than one would naively predict for a single electron transfer. Thus, the nontransferring electrons move a small distance in the opposite direction of the transferring electron. For the nanoparticle system, the excited state is much more polarizable than the ground state and the donating center is sufficiently negative that even in the CT state it is negatively charged. The negative donating center will polarize both the ground and excited states, but because the polarizability of the excited state is larger, the effect in the excited state will dominate. The net effect would be to decrease the polarization induced dipole-moment change and increase the observed charge-transfer distance.

The Stark spectra also allow one to calculate the electronic coupling between the metal–cyanide center and the TiO_2 on the basis of a two-state model (Table 3). The coupling for the

MPCT transitions is similar in magnitude to those observed between discrete molecular centers in intervalence transitions.^{22,52,54–56} The coupling strength calculated from the Stark spectra can be related back to the product of the DOS of the TiO_2 conduction-band states times the electronic coupling between the semiconductor and the metal cyanide.

The short distances for electron transfer estimated from the Stark spectra are consistent with the peak in the spectra being defined by differences in the electronic coupling for different levels in the TiO_2 nanoparticle. If the peak in the absorption spectra were due to changes in the DOS of the semiconductor, then one would expect that the MPCT would be primarily into states that are delocalized over the particle and the observed charge-transfer distance would be much larger. However, if the increased coupling between the complex and semiconductor states controls the shape of the absorption band, then the band shape would be dominated by only a few conduction-band levels and would more closely resemble the metal-to-metal charge-transfer spectra observed in dinuclear complexes. Thus, the Franck–Condon CT state while embedded in the conduction band of the particle is dominated by contributions from the titanium center that is attached to the CN bridge of the metal–cyanide complex. The dominant effect of the nanoparticle nature of the acceptor is that the polarization change is significantly larger than normally observed for dinuclear systems.

Conclusions

The new absorption features that occur when $Fe(CN)_6^{4-}$, $Ru(CN)_6^{4-}$, $Mo(CN)_6^{4-}$, or $W(CN)_6^{4-}$ bind to TiO_2 are shown to all involve metal-to-particle charge transfer. The energies of their absorptions suggest that the transition results in an electron being transferred into the conduction band at ≈ 0.5 eV above the band edge with the maximum in the absorption spectrum occurring for conduction-band states that have their largest contribution from the Ti center that is directly coordinated to the metal–cyanide complex. Electroabsorption (Stark) spectroscopy was used to study interfacial charge-transfer in the $M(CN)_n^{4-}/TiO_2$ systems. The average charge-transfer distances determined from the Stark spectra are similar for all of the metal–cyanide/ TiO_2 systems studied. The measurements indicate that the transition involves the transfer of an electron to a conduction-band state that is dominated by contributions from the Ti(IV) center coordinated to the metal–cyanide complexes. The transition does not result in the direct transfer of an electron into a state delocalized over the entire particle. Future work will include experiments to test the sensitivity of the transition to the energy of the conduction-band edge and to changes in the donating center.

Acknowledgment. B.S.B. acknowledges Dr. Norman Sutin's encouragement to build a Stark spectrometer and undertake studies of charge-transfer compounds using it. Specifically, we would like to thank him for detailed discussions and very helpful advice on this manuscript. We also thank Professor Harry B. Gray for the generous donation of $K_4[W^{IV}(CN)_8] \cdot H_2O$ and $K_4[Mo^{IV}(CN)_8] \cdot 2H_2O$. This work was supported by the Molecular Materials Research Center of the Beckman Institute at the California Institute of Technology and the National Science Foundation.

Note Added after ASAP Publication. This article was posted ASAP on April 3, 2007. Figure 1 has been revised. The corrected version was posted on May 30, 2007.

References and Notes

- (1) Fajardo, A. M.; Lewis, N. S. *Science* **1996**, 274, 969.
- (2) Fajardo, A. M.; Lewis, N. S. *J. Phys. Chem.* **1997**, 101, 11136.

- (3) Hamann, T. W.; Gstrein, F.; Brunschwig, B. S.; Lewis, N. S. *J. Am. Chem. Soc.* **2005**, *127*, 13949.
- (4) Hamann, T. W.; Gstrein, F.; Brunschwig, B. S.; Lewis, N. S. *J. Am. Chem. Soc.* **2005**, *127*, 7815.
- (5) Hamann, T. W.; Gstrein, F.; Brunschwig, B. S.; Lewis, N. S. *Chem. Phys.* **2006**, *326*, 15.
- (6) Creutz, C.; Brunschwig, B. S.; Sutin, N. *J. Phys. Chem. B* **2005**, *109*, 10251.
- (7) Creutz, C.; Brunschwig, B. S.; Sutin, N. *Chem. Phys.* **2006**, *324*, 244.
- (8) Creutz, C.; Brunschwig, B. S.; Sutin, N. *J. Phys. Chem.* **2006**, *110*, 25181.
- (9) Hagfeldt, A.; Grätzel, M. *Chem. Rev.* **1995**, *95*, 49.
- (10) Grätzel, M. *Nature* **2001**, *414*, 338.
- (11) Nazeeruddin, M. K.; Pechy, P.; Renouard, T.; Zakeeruddin, S. M.; Humphry-Baker, R.; Comte, P.; Liska, P.; Cevey, L.; Costa, E.; Shklover, V.; Spiccia, L.; Deacon, G. B.; Bignozzi, C. A.; Grätzel, M. *J. Am. Chem. Soc.* **2001**, *123*, 1613.
- (12) Nazeeruddin, M. K.; Kay, A.; Rodicio, I.; Humphrybaker, R.; Muller, E.; Liska, P.; Vlachopoulos, N.; Grätzel, M. *J. Am. Chem. Soc.* **1993**, *115*, 6382.
- (13) Ghosh, H. N.; Asbury, J. B.; Weng, Y.; Lian, T. *J. Phys. Chem. B* **1998**, *102*, 10208.
- (14) Vrachnou, E.; Vlachopoulos, N.; Grätzel, M. *Chem. Commun.* **1987**, 868.
- (15) Vrachnou, E.; Grätzel, M.; McEvoy, A. J. *J. Electroanal. Chem.* **1989**, *258*, 193.
- (16) Kushmerick, J. G.; Holt, D. B.; Pollack, S. K.; Ratner, M. A.; Yang, J. C.; Schull, T. L.; Naciri, J.; Moore, M. H.; Shashidhar, R. *J. Am. Chem. Soc.* **2002**, *124*, 10654.
- (17) Yang, M.; Thompson, D. W.; Meyer, G. J. *Inorg. Chem.* **2002**, *41*, 1254.
- (18) Umapathy, S.; McQuillan, A. J.; Hester, R. E. *Chem. Phys. Lett.* **1990**, *170*, 128.
- (19) Blackbourn, R. L.; Johnson, C. S.; Hupp, J. T. *J. Am. Chem. Soc.* **1991**, *113*, 1060.
- (20) Desilvestro, J.; Pons, S.; Vrachnou, E.; Grätzel, M. *J. Electroanal. Chem.* **1988**, *246*, 411.
- (21) Dobson, K. D.; McQuillan, A. J. *PCCP* **2000**, *2*, 5180.
- (22) Khoudiakov, M.; Parise, A. R.; Brunschwig, B. S. *J. Am. Chem. Soc.* **2003**, *125*, 4637.
- (23) Weng, Y. X.; Wang, Y. Q.; Asbury, J. B.; Ghosh, H. N.; Lian, T. *J. Phys. Chem. B* **2000**, *104*, 93.
- (24) Angelis, F. D.; Tilocca, A.; Selloni, A. *J. Am. Chem. Soc.* **2004**, *126*, 15024.
- (25) Rajh, T.; Nedeljkovic, J. M.; Chen, L. X.; Poluektov, O.; Thurnauer, M. C. *J. Phys. Chem. B* **1999**, *103*, 3515.
- (26) Redfern, P. C.; Zapol, P.; Curtiss, L. A.; Rajh, T.; Thurnauer, M. C. *J. Phys. Chem. B* **2003**, *107*, 11419.
- (27) Abuabara, S. G.; Rego, L. G. C.; Batista, V. S. *J. Am. Chem. Soc.* **2005**, *127*, 18234.
- (28) Coe, B. J.; Harris, J. A.; Brunschwig, B. S. *J. Phys. Chem. A* **2002**, *106*, 897.
- (29) Shin, Y.-G. K.; Brunschwig, B. S.; Creutz, C.; Sutin, N. *J. Phys. Chem.* **1996**, *100*, 8157.
- (30) Shin, Y.-G. K.; Brunschwig, B. S.; Creutz, C.; Sutin, N. *J. Am. Chem. Soc.* **1995**, *117*, 8668.
- (31) Liptay, W. Excited States. In *Excited States*; Lim, E. C., Ed.; Academic Press: New York, 1974; Vol. 1; p 129.
- (32) Shin, Y.-G. K.; Brunschwig, B. S.; Creutz, C.; Sutin, N. *J. Phys. Chem.* **1996**, *100*, 8157.
- (33) Bublitz, G. U.; Boxer, S. G. *Annu. Rev. Phys. Chem.* **1997**, 213.
- (34) Shin, Y.-G. K.; Brunschwig, B. S.; Creutz, C.; Sutin, N. *J. Phys. Chem.* **1996**, *100*, 8157.
- (35) Bard, A. J.; Roger Parsons; Jordan, J. *Standard Potentials in Aqueous Solution*; Marcel Dekker, Inc.: New York, 1985.
- (36) Billing, R.; Vogler, A. *J. Photochem. Photobiol., A* **1997**, *103*, 239.
- (37) Harris, L. A.; Wilson, R. H. *Annu. Rev. Mater. Sci.* **1978**, *8*, 99.
- (38) Duonghong, D.; Ramsden, J.; Grätzel, M. *J. Am. Chem. Soc.* **1982**, *104*, 2977.
- (39) Brunschwig, B. S.; Creutz, C.; Macartney, D. H.; Sham, T.-K.; Sutin, N. *Discuss. Faraday Soc.* **1982**, *74*, 113.
- (40) Brown, G. M.; Sutin, N. *J. Am. Chem. Soc.* **1979**, *101*, 883.
- (41) Marcus, R. A. *J. Phys. Chem.* **1990**, *94*, 1050.
- (42) CAChe, 6.1.12 ed.; Fujitsu, 2006.
- (43) Busani, T.; Devine, R. A. B. *Semicond. Sci. Technol.* **2005**, *20*, 870.
- (44) Gaal, D. A.; Hupp, J. T. *J. Am. Chem. Soc.* **2000**, *122*, 10956.
- (45) Gaal, D. A.; Hupp, J. T. Photo-Induced Electron Transfer Reactivity at Nanoscale Semiconductor-Solution Interfaces: Case Studies with Dye-Sensitized SnO₂-Water Interfaces. In *Semiconductor Photochemistry and Photophysics (Molecular and Supramolecular Photochemistry, 10)*; Ramamuth, V., Schatz, K. S., Eds.; Marcel Dekker: New York, 2003; p 89.
- (46) Kuciauskas, D.; Freund, M. S.; Gray, H. B.; Winkler, J. R.; Lewis, N. S. *J. Phys. Chem. B* **2001**, *105*, 392.
- (47) Sze, S. M. *Semiconductor Devices, Physics and Technology*, 2nd ed.; Wiley: New York, 2002.
- (48) Chen, Q.; Cao, H. H. *Chin. Phys.* **2004**, *13*, 2121.
- (49) Asahi, R.; Taga, Y.; Mannstadt, W.; Freeman, A. J. *Phys. Rev. B* **2000**, *61*, 7459.
- (50) Sakata, T.; Hashimoto, K.; Hiramotoff, M. *J. Phys. Chem.* **1990**, *94*, 3040.
- (51) Walters, K. A.; Gaal, D. A.; Hupp, J. T. *J. Phys. Chem. B* **2002**, *106*, 5139.
- (52) Karki, L.; Lu, H. P.; Hupp, J. T. *J. Phys. Chem.* **1996**, *100*, 15637.
- (53) Vance, F. W.; Karki, L.; Reigle, J. K.; Hupp, J. T.; Ratner, M. A. *J. Phys. Chem. A* **1998**, *102*, 8320.
- (54) Vance, F. W.; Slone, R. V.; Stern, C. L.; Hupp, J. T. *Chem. Phys.* **2000**, *253*, 313.
- (55) Bublitz, G. U.; Laidlaw, W. M.; Denning, R. G.; Boxer, S. G. *J. Am. Chem. Soc.* **1998**, *120*, 6068.
- (56) Vance, F. W.; Lemon, B. I.; Hupp, J. T. *J. Phys. Chem. B* **1998**, *102*, 10091.